Cell Metabolism
Article

Induction of the Mitochondrial NDUFA4L2 Protein by HIF-1α Decreases Oxygen Consumption by Inhibiting Complex I Activity

Daniel Tello,[1,5] Eduardo Balsa,[1,5] Bárbara Acosta-Iborra,[1] Esther Fuertes-Yebra,[1] Ainara Elorza,[1] Ángel Ordóñez,[1] María Corral-Escariz,[1] Inés Soro,[1] Elia López-Bernardo,[1] Ester Perales-Clemente,[2] Antonio Martínez-Ruiz,[1] José Antonio Enríquez,[2,3] Julián Aragonés,[1] Susana Cadenas,[1,4] and Manuel O. Landázuri[1,*]

[1]Servicio de Inmunología, Hospital Universitario de La Princesa, Universidad Autónoma de Madrid, Instituto de Investigación Sanitaria Princesa (IIS-IP), Madrid, 28006, Spain
[2]Centro Nacional de Investigaciones Cardiovasculares Carlos III (CNIC), Madrid, 28029, Spain
[3]Departamento de Bioquímica y Biología Molecular y Celular, Facultad de Ciencias, Universidad de Zaragoza, Zaragoza, 50013, Spain
[4]Departamento de Biología Molecular, Facultad de Ciencias, Universidad Autónoma de Madrid, Madrid, 28049, Spain
[5]These authors contributed equally to this work
*Correspondence: mortiz.hlpr@salud.madrid.org
DOI 10.1016/j.cmet.2011.10.008

SUMMARY

The fine regulation of mitochondrial function has proved to be an essential metabolic adaptation to fluctuations in oxygen availability. During hypoxia, cells activate an anaerobic switch that favors glycolysis and attenuates the mitochondrial activity. This switch involves the hypoxia-inducible transcription factor-1 (HIF-1). We have identified a HIF-1 target gene, the mitochondrial *NDUFA4L2* (NADH dehydrogenase [ubiquinone] 1 alpha subcomplex, 4-like 2). Our results, obtained employing NDUFA4L2-silenced cells and NDUFA4L2 knockout murine embryonic fibroblasts, indicate that hypoxia-induced NDUFA4L2 attenuates mitochondrial oxygen consumption involving inhibition of Complex I activity, which limits the intracellular ROS production under low-oxygen conditions. Thus, reducing mitochondrial Complex I activity via NDUFA4L2 appears to be an essential element in the mitochondrial reprogramming induced by HIF-1.

INTRODUCTION

Aerobic organisms have developed specific systems to deliver oxygen to cells in different anatomical locations. However, insufficient oxygen supply and the ensuing hypoxia is a hallmark of different pathological situations. In response to hypoxia, cells activate a metabolic program that reduces oxygen consumption by actively lowering mitochondrial oxidative phosphorylation (OXPHOS) activity, the main oxygen-consuming process in most cell types, accompanied by an increase in glucose uptake and the rate of glycolysis (Aragonés et al., 2008; Iyer et al., 1998; Kim et al., 2006; Papandreou et al., 2006). This hypoxic adaptation is due to the expression of genes triggered by hypoxia-inducible factors (HIFs) (Aragonés et al., 2009). HIFs are master transcription factors regulated in an O_2-dependent manner by a family of prolyl hydroxylases (PHDs), which use O_2 as a substrate to hydroxylate HIF-α subunits in conditions of normoxia (Kaelin and Ratcliffe, 2008). These hydroxylated substrates are then ubiquitinated after recognition by VHL, and they are degraded by the proteasome. By contrast, PHD activity is inhibited in hypoxic conditions, and accordingly, HIF-α subunits accumulate, heterodimerize with HIF-β, and activate the expression of HIF-dependent target genes (Schofield and Ratcliffe, 2004; Semenza, 2004, 2009).

Among the genes whose expression is upregulated by HIFs are glucose transporters, like *GLUT1*, as well as key enzymes involved in glycolysis (Iyer et al., 1998). The *PDK1* and *PDK3* genes that code for pyruvate dehydrogenase (PDH) kinases are also upregulated, which results in increased phosphorylation and inactivation of PDH, the enzyme that converts pyruvate to acetyl-CoA (Kim et al., 2006; Lu et al., 2008; Papandreou et al., 2006). This process limits the substrate available for the tricarboxylic acid cycle (TCA) and thus for OXPHOS activity. Mitochondrial respiration is also regulated by additional mechanisms that maximize respiratory efficiency under conditions of reduced O_2 availability. Genes that regulate cytochrome *c* oxidase (the ETC Complex IV that reduces O_2 to H_2O) are also regulated by HIFs, including *COX4-2* isoform and the *LON* protease, which produces a switch from isoform COX4-1 to COX4-2 that optimizes the efficiency of respiration under hypoxic conditions (Fukuda et al., 2007).

Complex I (NADH:ubiquinone oxidoreductase) is the largest and least understood component of the respiratory chain. This complex catalyzes the first step in the electron transport chain (ETC), transferring electrons from NADH to a noncovalently bound flavin mononucleotide (FMN) and then, via a series of iron-sulfur clusters (FeS), to the final ubiquinone acceptor. Complex I consists of 45 different subunits that are assembled into a structure of ~1 MDa, and while 7 subunits are encoded by mitochondrial DNA, the remaining 38 are coded for by the nuclear genome (Carroll et al., 2006). The activity of the Complex I is affected by hypoxia, either through posttranslational modification (Frost et al., 2005) or the reduced expression of mitochondrial genes (Chan et al., 2009). Here we report that HIF-1 induces the expression of the NADH dehydrogenase (ubiquinone) 1 alpha subcomplex subunit 4-like 2 gene (*NDUFA4L2*, also called

NADH-ubiquinone oxidoreductase MLRQ subunit homolog [*NUOMS*]), cataloged as a component of ETC Complex I due to its high sequence identity with *NDUFA4*. It was previously described using mRNA array technology that NDUFA4L2 is overexpressed in VHL-deficient cell lines and tumors (Favier et al., 2009; Papandreou et al., 2006), as well as in neuroblastoma cells in hypoxia (Fredlund et al., 2008) and in pathophysiological conditions like rheumatoid arthritis (Andreas et al., 2009). Although the physiological function of this protein remains unclear, we show here that it is involved in lowering mitochondrial oxygen consumption and Complex I activity, thereby reducing ROS production. This provides a point in the regulation of mitochondrial activity that can reprogram Complex I activity under low-oxygen conditions.

RESULTS

Hypoxia Induces the Mitochondrial Protein NDUFA4L2 in Primary Cultures and Tumor Cells In Vitro as well as In Vivo

We hypothesized that, as the principal electron acceptor, Complex I could be a key regulatory point in the control of the ETC during hypoxia. To identify Complex I components that might be regulated by moderate hypoxia, we used an mRNA array to analyze the expression of genes in HeLa cells maintained for short periods of time (6 hr) in 1% O_2. We detected the expression of 44 genes of Complex I in the array: 40 genes encoded by nuclear DNA and 4 encoded in the mitochondria (*ND1*, *ND2*, *ND3*, and *ND6*). Of all these genes, only *NDUFA4L2* was clearly induced by hypoxia, whereas the other genes encoded by nuclear DNA remained unchanged (Table S1). By contrast and as described previously (Piruat and López-Barneo, 2005), the other mitochondrially encoded genes underwent a marked downregulation in these hypoxic conditions (Table S1). It is important to note that *NDUFA4L2* gene is strongly induced by hypoxia. In fact, it appears among the first 12 genes more induced by hypoxia in the mRNA study (Table S2).

These microarray data were validated by RT-PCR on mRNA isolated from HeLa and PC-12 cells exposed to hypoxia. Indeed, RT-PCR assays confirmed that NDUFA4L2 expression was strongly upregulated in response to hypoxia (Figure 1A), while such conditions did not change the levels of other Complex I genes encoded in the nucleus, such as *NDUFA4*, *NDUFAB1*, or *NDUFB4*, although *ND1* and *ND6* expression was downregulated (Figure S1A). Upregulation of *NDUFA4L2* expression was also observed in HUVEC and cardiomyocytes subjected to hypoxia and after treatment with PHD inhibitors such as dimethyloxaloylglycine (DMOG) and deferroxamine (Figure 1B). The efficacy of hypoxia and DMOG in these experiments was corroborated by the marked upregulation of previously recognized HIF target genes such as *PHD3*, *BNIP3*, and *GLUT1* (Figure S1B). In addition, NDUFA4L2 expression was induced in brain tissue of mice exposed to 7.5% O_2 for 18 hr (Figure 1C). An increase in NDUFA4L2 protein was also evident in response to hypoxia in different cell types and brain tissue (Figure 1D) with an antibody specific to this protein that did not recognize the homologous NDUFA4 protein (Figure S1C). Moreover, the increase in NDUFA4L2 protein induced by hypoxia was evident in cardiomyocytes when assessed by immunofluorescence (Figure 1E).

We analyzed the cellular localization of NDUFA4L2 in normoxic and hypoxic conditions. A bioinformatics approach predicted that NDUFA4L2 would be localized in mitochondria (Table S3), and this prediction was then confirmed experimentally by analyzing mitochondrial and cytoplasmic fractions from HeLa cells. NDUFA4L2 was clearly enriched in the mitochondrial fraction under hypoxic conditions (Figure 1F), and immunofluorescence showed a clear colocalization of NDUFA4L2 and cytochrome *c* in HL-1 cells (Figure 1G), as well as the colocalization of NDUFA4L2 and the mitochondria-selective dye MitoTracker in HeLa cells (Figure S1D). These results confirmed the mitochondrial location of NDUFA4L2.

HIF-1α Regulates NDUFA4L2 Induction

To investigate whether hypoxia-induced *NDUFA4L2* expression was mediated by HIF transcription factors, we first silenced HIF-1β, the common partner of HIF-1α and HIF-2α, thereby impairing the canonical HIF transcriptional response. Interference of HIF-1β expression abolished the induction of *NDUFA4L2* during hypoxia (Figure 2A), as well as the response of *PHD3* (included as a control of HIF-target gene) (Figure S2A), indicating that HIF transcriptional activity is essential for *NDUFA4L2* induction.

To study the specific role of HIF-1α and HIF-2α in the response of *NDUFA4L2* to hypoxia, we performed RNA interference assays in human renal carcinoma RCC4 cells that constitutively stabilize HIF-1α and HIF-2α through the absence of VHL. Likewise, the response of NDUFA4L2 was also assessed in RCC4/VHL cells in which VHL expression was restored, and hence both HIF-1α and HIF-2α were exclusively upregulated in response to hypoxia. In line with the role of HIF activity in *NDUFA4L2* regulation, there was a robust upregulation of *NDUFA4L2* in hypoxic RCC4/VHL cells, whereas there was marked and constitutive *NDUFA4L2* expression in normoxic RCC4 cells that was only minimally upregulated in hypoxic conditions (Figure 2B). HIF-1α interference abrogated the expression of *NDUFA4L2* in both normoxic and hypoxic RCC4 cells (Figure 2B), as well as hypoxia-driven *NDUFA4L2* expression in RCC4/VHL cells (Figure 2B). By contrast, HIF-2α interference did not affect the expression of *NDUFA4L2* in RCC4/VHL cells exposed to hypoxia, and no significant effect was observed in RCC4 cells in either normoxic or hypoxic conditions (Figure 2B). The control experiments for the interference assays showed a specific reduction of *HIF-1α* or *HIF-2α* mRNA expression (Figure S2B).

We further confirmed these data in mouse embryonic fibroblasts (MEFs) from Hif-$1\alpha^{+f/+f}$/Cre conditional mice in which HIF-1α was lost after tamoxifen treatment. As a control, we employed tamoxifen Hif-$1\alpha^{+/+}$/Cre MEFs that lacked the CRE recombination sites required for HIF-1α ablation. The hypoxic induction of *Ndufa4l2* expression as well as that of the HIF target gene *Phd3* were only abrogated in Hif-$1\alpha^{+f/+f}$/Cre conditional MEFs following tamoxifen exposure, whereas they were still expressed in Hif-$1\alpha^{+/+}$/Cre MEFs (Figures 2C and S2C). Hence, the hypoxic induction of *Ndufa4l2* appeared to be mostly mediated by HIF-1α.

To identify possible hypoxia response elements (HREs) responsible for the induction of *NDUFA4L2*, the proximal promoter region (intron 1) of *NDUFA4L2* was analyzed, identifying

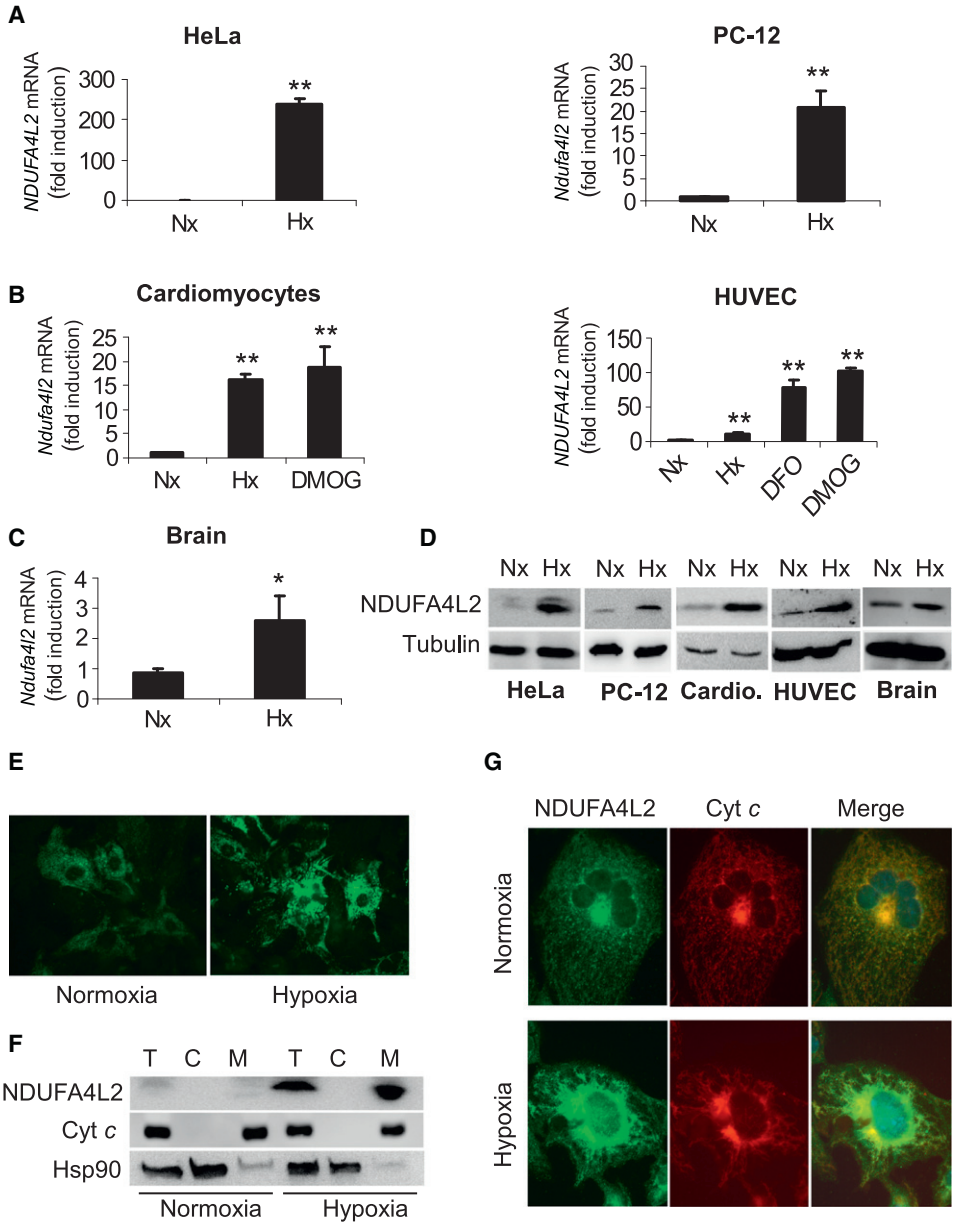

Figure 1. NDUFA4L2 Localizes to Mitochondria and Is Induced in Tumor Cells, in Primary Cultures, and In Vivo by Hypoxia

(A–C) Quantitative RT-PCR analysis of *NDUFA4L2* mRNA expression relative to the values in normoxia. HeLa, PC-12, cardiomyocytes, and HUVEC were cultured under conditions of normoxia or hypoxia (1% O_2) for 6 (HeLa) or 18 hr (PC-12, cardiomyocytes, HUVEC) (A and B). DMOG was added at 1 mM (cardiomyocytes) or 0.1 mM (HUVEC), and deferroxamine (DFO) was added at 0.2 mM in HUVEC (n = 3). Brain tissue from mice exposed to normoxic (n = 8) or hypoxic (7.5% O_2; n = 7) conditions for 18 hr is shown in (C).

(D) Immunoblot assay of NDUFA4L2 protein in HeLa, PC-12, HUVEC, or rat cardiomyocytes cultured under normoxic or hypoxic conditions (1% O_2 for cell cultures), as well as in brain tissue of mice subjected to hypoxia (7.5% O_2) for 18 hr. Tubulin is shown as a loading control. The images are representative of at least three experiments.

(E) Immunofluorescence showing the increase in NDUFA4L2 protein levels in rat cardiomyocytes exposed to normoxia or hypoxia (1% O_2) for 18 hr, with respect to those maintained in normoxic conditions. The images shown are representative of three experiments.

(F) Immunoblot assay of NDUFA4L2 in total cell (T), cytoplasmic (C), and mitochondrial (M) protein extracts from HeLa cells cultured under normoxic or hypoxic conditions (1% O_2) for 18 hr. Cytochrome *c* was assayed as a mitochondrial marker. The images shown are representative of three experiments.

(G) Immunofluorescence of HL-1 cells exposed to normoxia or hypoxia (1% O_2) for 18 hr. Images show staining for NDUFA4L2 (left panel, green) and cytochrome *c* (middle panel, red) and an overlay of the two signals (right panel). The images shown are representative of three experiments. See also Figure S1. n > 3; mean ± SEM; *p < 0.05; **p < 0.01.

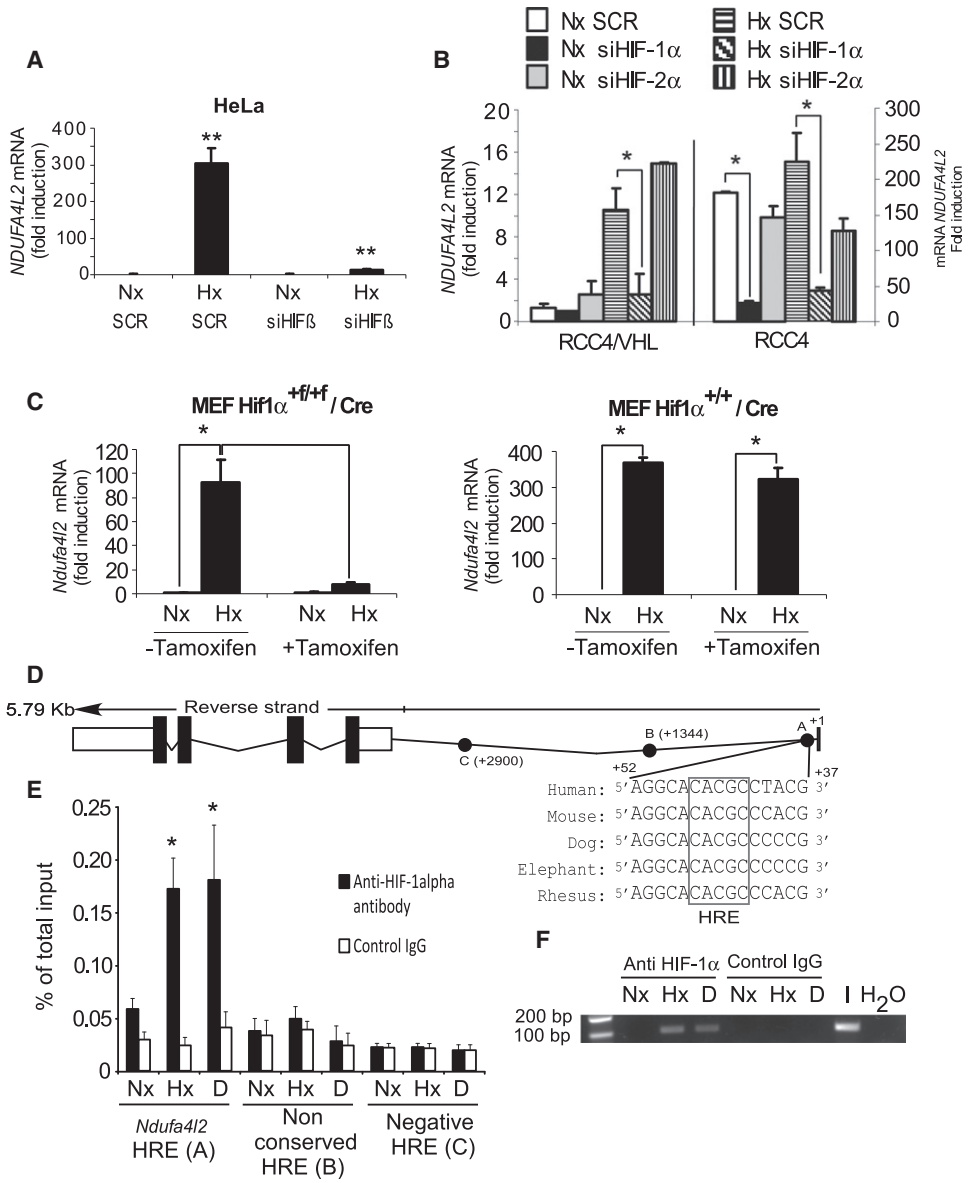

Figure 2. *NDUFA4L2* Induction Is Mediated by HIF-1α

(A) HeLa cells transfected with siRNA against HIF-β or a scramble control were cultured under normoxic or hypoxic (1% O_2) conditions for 24 hr. *NDUFA4L2* mRNA levels were quantified by real-time RT-PCR.

(B) VHL-deficient RCC4 cells or RCC4/VHL cells were transfected with siRNA against HIF-1α, HIF-2α, or a scramble control and exposed under normoxic or hypoxic conditions (1% O_2) for 24 hr. *NDUFA4L2* mRNA levels were quantified by real-time RT-PCR and are expressed relative to normoxic RCC4/VHL.

(C) Hif-1$\alpha^{+/+}$/Cre MEFs and Hif-1$\alpha^{+f/+f}$/Cre MEFs in the presence or absence of tamoxifen (1 μM) were cultured under normoxic or hypoxic conditions (1% O_2) for 18 hr. *NDUFA4L2* mRNA levels were quantified by real-time RT-PCR.

(D) Schematic representation of the human *NDUFA4L2* gene and the nucleotide sequences matching the consensus hypoxia response element (HRE) from five mammalian genes, indicating the regions A-B-C analyzed in the ChIP assay.

(E) ChIP assay of HIF-1α binding to the human *NDUFA4L2* gene in HeLa cells cultured in normoxic or hypoxic conditions (1% O_2) or exposed to DMOG (0.1 mM) for 6 hr. RT-PCR quantification is shown of regions A (putative NDUFA4L2 HRE), B (nonconserved HRE), and C (negative HRE) after immunoprecipitation with HIF-1α or a control antibody, represented as the percentage of that quantified in the total input DNA.

(F) Representative gel of DNA amplified in the ChIP assays shown in (E). See also Figure S2. n > 3; mean ± SEM; *p < 0.05; **p < 0.01.

two putative HREs at +43 and +1344 (Figure 2D). The +43 site is highly conserved between different species, unlike the +1344 site. Chromatin immunoprecipitation (ChIP) assays were performed on HeLa cells grown under normoxic or hypoxic conditions and after treatment with DMOG. To evaluate HIF-1α binding to *NDUFA4L2* regulatory sequences, quantitative PCR (qPCR) was performed using specific primers for the putative HRE site (A), the nonconserved HRE site (B), and a negative site (C). ChIP assays for *PDK1*, a well-known HIF-1α target, were also performed as a positive control (Figure S2D). HIF-1α

binding to the *NDUFA4L2* proximal promoter containing conserved HRE site (A) was strongly induced by hypoxia and DMOG treatment (Figure 2E), but not to the nonconserved HRE site (B) or the negative control region (C). The sequence amplified by qPCR had the expected size (Figure 2F). Taken together, these results suggest that *NDUFA4L2* is a direct HIF-1 target gene.

NDUFA4L2 Is Involved in the Hypoxia-Induced Decrease in Oxygen Consumption and Prevents Increases in Membrane Potential and ROS Production during Hypoxia

To test whether NDUFA4L2 is involved in the regulation of mitochondrial activity in hypoxia, we first determined the oxygen consumption in HeLa cells in which NDUFA4L2 was silenced by specific siRNA. In these experiments, *NDUFA4L2* expression was typically reduced by 80% in hypoxic conditions (Figure S3A) while *NDUFA4* mRNA levels were not affected by the siNDUFA4L2 (Figure S3B), highlighting the specificity of the interference of NDUFA4L2. Indeed, NDUFA4L2 interference reduced its protein expression in both normoxic and hypoxic conditions (Figure 3A), whereas the expression levels of proteins from other ETC complexes were unaffected by NDUFA4L2 interference (Figure S3C). Oxygen consumption decreased approximately 42% in hypoxic conditions when compared to normoxia in control HeLa cells (Figure 3B). However, oxygen consumption only decreased by 27% in hypoxic conditions when NDUFA4L2 was silenced in HeLa cells and when compared to control cells in normoxic conditions (Figure 3B). In normoxia, NDUFA4L2 silencing increased oxygen consumption by only 10%, probably due to the low normoxic levels of NDUFA4L2. We also tested whether transient overexpression of NDUFA4L2 might decrease oxygen consumption by using a pCMV-NDUFA4L2 vector to achieve expression levels similar to those obtained in hypoxia (Figures 3C and S3D). Transient overexpression of NDUFA4L2 decreased oxygen consumption in HeLa cells by approximately 20% (Figure 3D). Hence, we conclude that during hypoxia, NDUFA4L2 induction decreases oxygen consumption.

Since attenuation of mitochondrial activity in hypoxia may be a compensatory mechanism to keep mitochondrial ROS under control, we wondered whether hypoxia-driven NDUFA4L2 upregulation could also participate in this antioxidant response. Previous studies used the fluorescent dye H_2DCFDA and flow cytometry to demonstrate an increase of mitochondrial ROS production when cells are exposed to low O_2 tensions (Brunelle et al., 2005; Guzy et al., 2005; Mansfield et al., 2005). Accordingly, we observed increased H_2DCFDA fluorescence in HeLa cells exposed to hypoxia (1% O_2) that was exacerbated when NDUFA4L2 was silenced (Figure 3E). Similar data were obtained using the mitochondrial superoxide indicator MitoSOX (Figure 3F), which points to the mitochondrial origin of this increased superoxide production, probably from respiratory complexes. Increased ROS production in the absence of NDUFA4L2 during hypoxia correlated with an increased mitochondrial membrane potential in these conditions (Figure 3G). Conversely, NDUFA4L2 overexpression significantly decreased membrane potential compared to cells expressing the empty vector (Figure 3H).

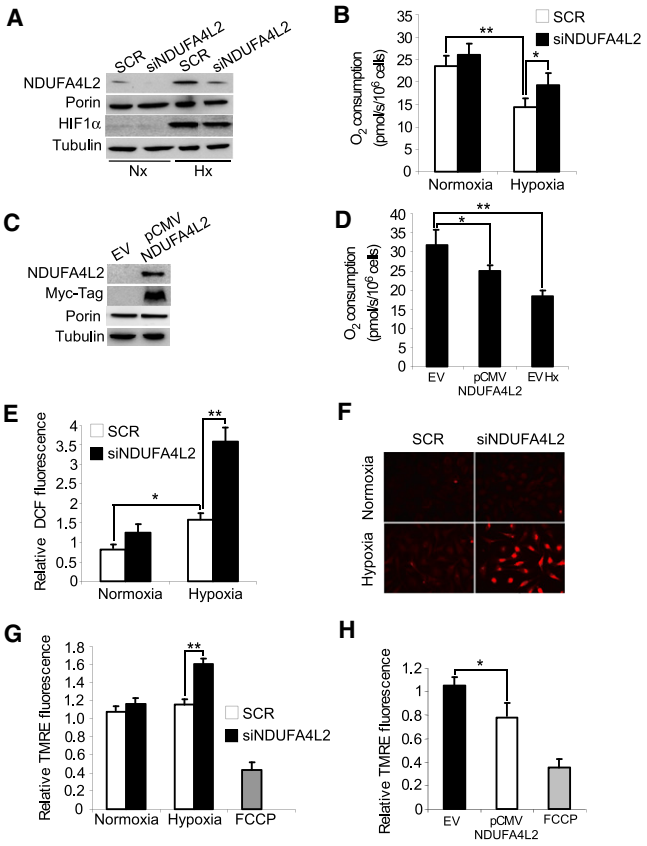

Figure 3. NDUFA4L2 Decreases Oxygen Consumption, Membrane Potential, and ROS Production in Hypoxia

(A–D) HeLa cells were transfected with a scramble control or NDUFA4L2 siRNA and exposed to normoxic or hypoxic (1% O_2) conditions for 18–24 hr. Immunoblot analysis of NDUFA4L2 and HIF-1α protein levels using tubulin and mitochondrial porin as loading controls is shown in (A). The images are representative of four independent experiments. Oxygen consumption rates were measured by high-resolution respirometry (B). HeLa cells were transfected with the empty vector (EV) or pCMV-NDUFA4L2 and then exposed to normoxic or hypoxic (1% O_2) conditions for 24 hr (C and D). Immunoblot analysis of NDUFA4L2 and myc-tagged protein levels using tubulin and mitochondrial porin as loading controls are shown (C). The images are representative of four independent experiments. Oxygen consumption rates were measured by high-resolution respirometry (D).

(E) Relative DCF fluorescence as a measure of intracellular hydrogen peroxide levels.

(F) Representative images of four independent experiments showing MitoSOX intensity as a measure of mitochondrial superoxide levels.

(G and H) Mitochondrial membrane potential was determined with the fluorescent probe TMRE and expressed relative to the control cells in normoxia. FCCP was used as a positive control of mitochondrial membrane depolarization (n > 3; mean ± SEM; *p < 0.05; **p < 0.01).

The Hypoxia-Induced Decrease in Oxygen Consumption via NDUFA4L2 Occurs through Complex I Inhibition

Given that NDUFA4L2 appears to be a mitochondrial protein involved in the downregulation of hypoxia-induced oxygen consumption, and that it likely belongs to the NDUFA4 subunit family of Complex I, we wondered whether NDUFA4L2 might be involved in actively regulating Complex I activity. We found that, when compared to normoxic conditions, Complex I activity

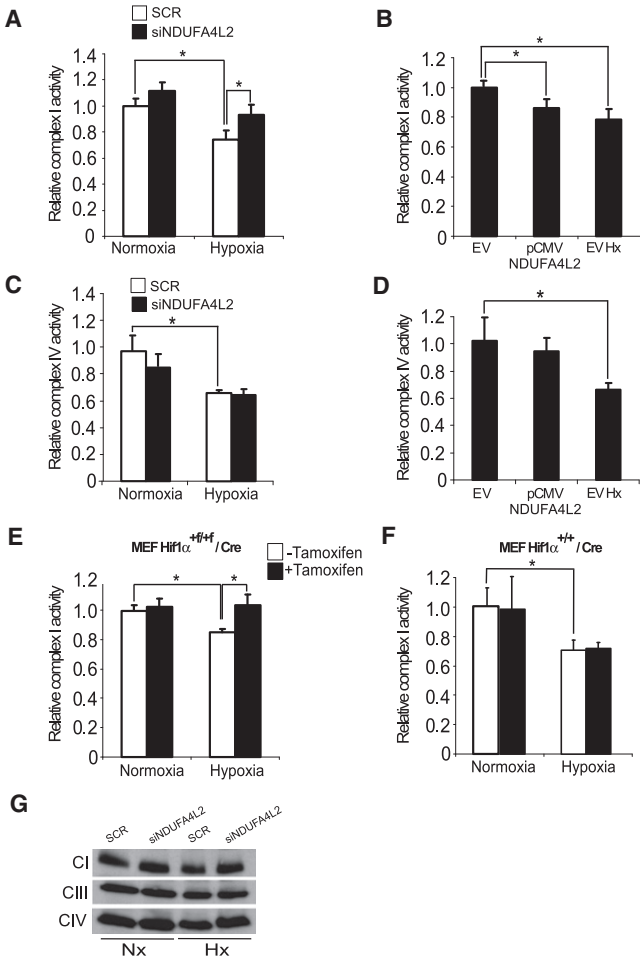

Figure 4. NDUFA4L2 Decreases Complex I Activity in Hypoxia

(A and B) Complex I activity was measured in HeLa cells transfected with a scramble control or NDUFA4L2 siRNA (A) or with the empty or pCMV-NDUFA4L2 vector (B), then exposed to normoxic or hypoxic (1% O_2) conditions for 24 hr.

(C and D) Complex IV activity was measured in HeLa cells transfected with a scramble control or NDUFA4L2 siRNA (C) and the empty or pCMV-NDUFA4L2 vector (D), then exposed to normoxic or hypoxic (1% O_2) conditions for 24 hr.

(E and F) Complex I activity was measured in Hif-1$\alpha^{+f/+f}$/Cre (E) or Hif-1$\alpha^{+/+}$/Cre MEFs (F) maintained in the presence or absence of tamoxifen (1 μM) for 48 hr and cultured under normoxic or hypoxic (1% O_2) conditions for 18 hr.

(G) Blue native PAGE (BN-PAGE) analysis of the mitochondrial OXPHOS Complex I (NDUFA9), Complex III (Core 2), and Complex IV (Col) from scramble and NDUFA4L2 siRNA HeLa cells exposed to normoxic or hypoxic (1% O_2) conditions for 24 hr (n > 3; mean ± SEM; *p < 0.05; **p < 0.01).

decreased ~20% in HeLa cells exposed to hypoxia (1% O_2 for 24 hr), although it did not when NDUFA4L2 expression was silenced (Figure 4A). Moreover, transient overexpression of NDUFA4L2 decreased Complex I activity in normoxic conditions (Figure 4B), demonstrating that NDUFA4L2 regulates Complex I under low-oxygen conditions.

To study the specificity of the effects of NDUFA4L2 on Complex I, we also measured Complex IV activity. Hypoxia (1% O_2 for 24 hr) induced a 38% decrease in Complex IV activity in HeLa cells (Figure 4C), but the silencing of NDUFA4L2 expression in hypoxia or its overexpression in normoxia did not affect Complex IV activity (Figures 4C and 4D). Similar results were obtained when Complex IV activity was determined spectrophotometrically (data not shown). Hence, NDUFA4L2 appears to affect ETC activity by specifically inhibiting Complex I. Since our results indicate that *NDUFA4L2* is a HIF-1α-dependent gene involved in the downregulation of Complex I activity in hypoxia, we further studied the role of HIF-1 in regulating Complex I. As expected, there was no decrease in Complex I activity following hypoxia in tamoxifen-treated Hif-1$\alpha^{+f/+f}$/Cre MEFs in which HIF-1α was ablated (Figure 4E). By contrast, a decrease in Complex I activity similar to that seen in HeLa cells was evident in tamoxifen-treated Hif-1$\alpha^{+/+}$/Cre MEFs (~20%) (Figure 4F). These results suggest that the HIF-1α-induced increase in NDUFA4L2 expression decreased oxygen consumption through the specific inhibition of mitochondrial Complex I activity.

Complex I activity can be modulated by its assembly (Vogel et al., 2005). We hypothesized that hypoxia-induced NDUFA4L2 could affect Complex I assembly. To test this possibility, we performed Blue native PAGE (BN-PAGE) in order to analyze the status of mitochondrial complexes. Neither hypoxia nor NDUFA4L2 silencing modified Complex I content, thus ruling out the involvement of NDUFA4L2 in the Complex I assembly process (Figure 4G).

Silencing of NDUFA4L2 Impairs Cell Proliferation in Hypoxia by Increasing Mitochondrial ROS Generation

While the absence of NDUFA4L2 does not significantly affect cell proliferation in normoxic conditions (Figure 5A), viable hypoxic NDUFA4L2-silenced HeLa cells proliferated at a slower rate than hypoxic control cells (Figure 5B). This slower proliferation was evident by both cell counting and by direct observation under the microscope (Figure 5C); it was also observed in other cell types such as HUVEC, UCD-Mel-N, and SKOV3 cells (Figure S4A). NDUFA4L2-silenced cells did not show either increased caspase-3 cleavage (Figure 5D) or changes in propidium iodide incorporation (Figure 5E), excluding the possibility that NDUFA4L2 silencing impaired cell proliferation by activating apoptosis. Additional studies showed that the capacity of hypoxic HeLa cells to form colonies in soft agar was affected when NDUFA4L2 was silenced, with a decrease in both the size and the number of colonies (Figure 5F). In order to investigate whether ROS overproduction in NDUFA4L2-silenced HeLa cells during hypoxia was responsible for the impairment in cell proliferation, we tested the effects of two different antioxidants, N-acetylcysteine (NAC) and MitoQ (an antioxidant targeted to mitochondria), on cell proliferation. Cell proliferation was restored when NDUFA4L2-silenced HeLa cells were treated with MitoQ in hypoxia (Figure 5G). This effect was also observed with NAC (Figure S4B), suggesting that exacerbated ROS production may be involved in the impairment of cell viability under hypoxia. Indeed, an increase in ROS production was detected in NDUFA4L2-silenced cells exposed to hypoxia using the mitochondrial superoxide indicator MitoSOX (Figure 5H). This increase was completely prevented by incubation with MitoQ (Figure 5H).

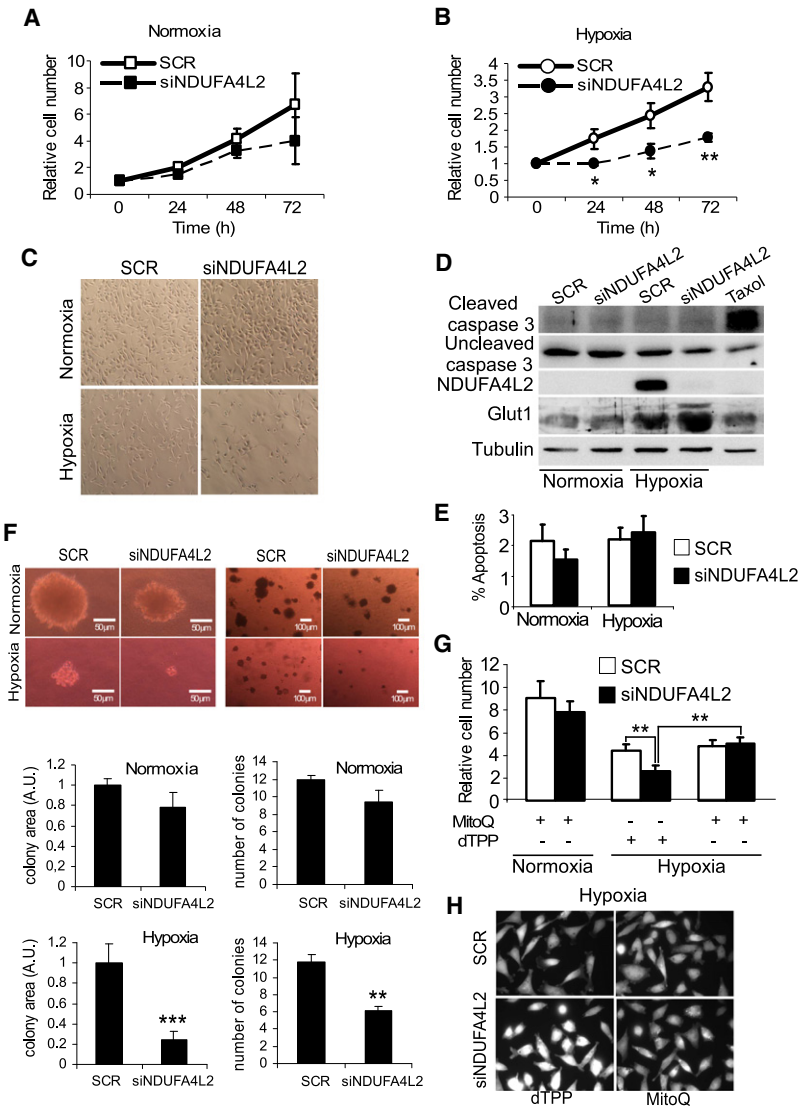

Figure 5. Reduced Hypoxic Levels of NDUFA4L2 Impair Cell Proliferation

(A and B) Growth curves of HeLa cells transfected with a scramble control or NDUFA4L2 siRNA in normoxic (A) and hypoxic (0.5% O_2) (B) conditions for different periods of time.

(C) Microscope images showing the density of HeLa cell cultures transfected with a scramble control or NDUFA4L2 siRNA and maintained under normoxic (21% O_2) or hypoxic (0.5% O_2) conditions for 72 hr.

(D) HeLa cells were transfected with either a scramble control or NDUFA4L2 siRNA and cultured under normoxic (21% O_2) or hypoxic (0.5% O_2) conditions for 72 hr, and the cell lysates were assayed in immunoblots that were probed with antibodies against NDUFA4L2, uncleaved caspase-3, and cleaved caspase-3. Glut1 was used as a positive control of hypoxic gene induction and tubulin as a loading control. Taxol was used as positive control of apoptosis.

(E) Scramble control or NDUFA4L2 siRNA HeLa cells maintained in normoxic (21% O_2) or hypoxic (0.5% O_2) conditions for 72 hr. The absolute value of apoptosis was measured by flow cytometry in cells stained with propidium iodide, as described in the Experimental Procedures.

(F) Image of colony formation by HeLa cells transfected with a scramble control or NDUFA4L2 siRNA in normoxic and hypoxic (0.5% O_2) conditions in soft agar for 15 days. Both size and number of colonies were quantified.

(G) Growth of HeLa cells transfected with a scramble control or NDUFA4L2 siRNA in normoxic and hypoxic (0.5% O_2) conditions with or without 0.5 μM MitoQ (0.5 μM dTPP was used as control of MitoQ) at 72 hr.

(H) Fluorescence microscopy images of hypoxic (0.5% O_2) cultured scramble and siNDUFA4L2 HeLa cells treated either with 0.5 μM MitoQ or 0.5 μM dTPP ($n > 3$; mean ± SEM; *$p < 0.05$; **$p < 0.01$).

Cell-cycle analysis showed that hypoxic NDUFA4L2-silenced HeLa cells had increased early S phase and decreased late S phase compared to scramble control cells (Figure S4C). Since NDUF4L2-silenced HeLa cells present ROS overproduction in hypoxia, and ROS can increase the phosphorylation of histone H2AX, a marker of cell stress (Driessens et al., 2009), we then analyzed the phosphorylation of H2AX histone. We observed increased phosho-H2AX levels in hypoxia when NDUFA4L2 was interfered (Figure S4D), suggesting that the lack of NDUFA4L2 in hypoxia produces cell stress.

It has been described that both the downregulation of the iron-sulfur cluster assembly proteins (ISCU1/2) via miR-210 and the upregulation of PDK1 are implicated in ROS control and cell viability in hypoxia (Chan et al., 2009; Chen et al., 2010; Favaro et al., 2010; Kim et al., 2006; Papandreou et al., 2006). To investigate the relative contribution of these effects to HeLa hypoxic adaptation, we performed cell proliferation assays. We only observed a decrease in ISCU1/2 protein at times over 24 hr at 0.5% (Figure S5A) but not in the milder hypoxic conditions (1% O_2). Furthermore, the overexpression of ISCU1/2 did not affect HeLa cell proliferation in hypoxia (0.5% O_2) at 72 hr (Figure S5B). In addition, HeLa cells in which PDK1 was silenced by specific siRNA (Figure S5C) showed a decrease in proliferation under hypoxia (0.5% O_2) at 72 hr (Figure S5D) similar to that observed in NDUFA4L2-silenced cells, suggesting that both NDUFA4L2 and PDK1 play an important role in ROS control and cell proliferation in our system conditions.

MEFs Obtained from NDUFA4L2 Knockout Mice Exhibit Higher Oxygen Consumption and Complex I Activity in Hypoxia Than Wild-Type MEFs

In order to gain further insight into the role of NDUFA4L2 on hypoxia-induced mitochondrial reprogramming, we generated NDUFA4L2 knockout (KO) mice. We initially planned to isolate primary cell cultures from NDUFA4L2-deficient adult mice. However, we found that homozygous *Ndufa4l2* gene inactivation results in perinatal lethality, which demonstrates an essential biological role of NDUFA4L2 in development that will be further explored in future studies. Therefore, we isolated NDUFA4L2-deficient MEFs and the corresponding wild-type controls from E12.5–14.5 embryos generated from NDUFA4L2$^{+/-}$ breeding pairs. In order to validate these MEF cultures, we analyzed the

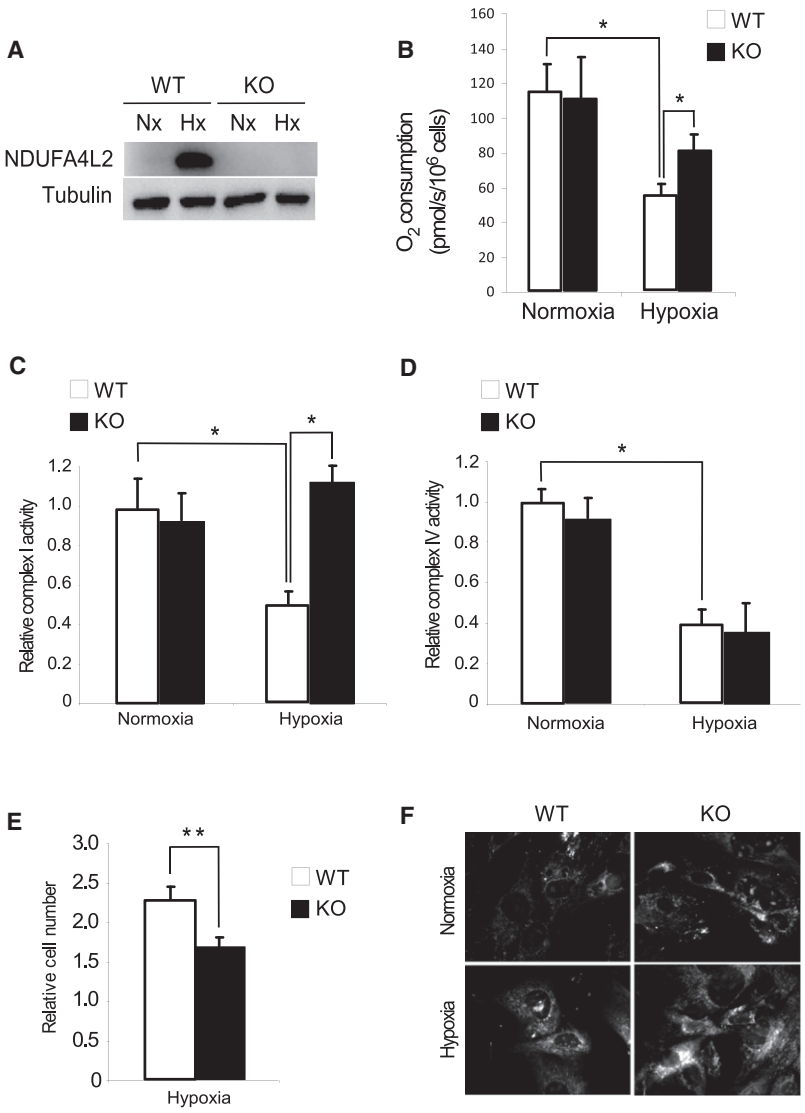

Figure 6. Analysis of NDUFA4L2-Deficient MEFs

(A–D) WT and KO MEFs were exposed to 0.5% hypoxia 24 hr prior to subsequent analysis. Immunoblot analysis showing the total deficiency of NDUFA4L2 is shown in (A). Tubulin was used as a loading control. Oxygen consumption rates were measured by high-resolution respirometry (Oxygraph 2k) (B). Complex I (C) and Complex IV (D) activities were measured spectrophotometrically and expressed relative to citrate synthase values.

(E) Relative growth rates of WT and KO NDUFA4L2 MEFs cultured in hypoxia (0.5% O_2).

(F) Representative images of three independent experiments showing MitoSOX intensity as a measure of mitochondrial superoxide levels (n > 3 mean ± SEM; *p < 0.05, **p < 0.01).

expression of NDUFA4L2. Western blot analysis confirmed that NDUFA4L2 increased in hypoxia in MEFs from wild-type mice only (Figure 6A). We determined oxygen consumption in MEFs obtained from NDUFA4L2 KO and wild-type mice (Figure 6B). Confirming results obtained in HeLa cells, MEFs from NDUFA4L2 KO mice showed increased respiration rate in hypoxia compared to wild-type mice (Figure 6B). The activity of Complex I in hypoxia was higher in MEFs from KO mice than in those from wild-type mice, confirming the results obtained in HeLa cells (Figure 6C). In contrast, the activity of Complex IV in hypoxia was similarly decreased in both types of MEFs (Figure 6D). The expression level of respiratory complexes was studied by BN-PAGE using DDM (n-dodecyl beta-D-maltoside), obtaining the same result as in HeLa cells (data not shown). In addition, MEFs from NDUFA4L2 KO mice exhibited a lower proliferation rate than those from wild-type mice when cultured under hypoxia (Figure 6E), and this lower proliferation correlated with increased ROS production under hypoxic conditions (Figure 6F).

NDUFA4 Paralogue Is Repressed under Hypoxia at the Protein Level

It is established that a COX4-2 to COX4-1 subunit substitution takes place at Complex IV during hypoxia (Fukuda et al., 2007). The paralogue proteins NDUFA4L2 and NDUFA4 derive from the same ancestral gene, share more than 65% in their amino acid sequence, and have been suggested to be part of mitochondrial Complex I (Walker et al., 1992). Since *NDUFA4* mRNA levels do not change in hypoxia up to 48 hr (Figure 7A), we investigated the fate of the protein under hypoxia. We found that NDUFA4 protein decreases in hypoxic cells while NDUFA4L2 protein expression increases in hypoxic conditions (Figure 7B). We also explored whether NDUFA4L2 levels would be responsible for the downregulation of NDUFA4. NDUFA4 protein levels decreased in hypoxia even when NDUFA4L2 was silenced (Figure 7C), and its expression in normoxia was unaffected by NDUFA4L2 overexpression (Figure 7D). NDUFA4 protein decreases to the same extent in NDUFA4L2 KO MEFs, demonstrating that both events occur independently (Figure 7E). Collectively, all these data indicate that NDUFA4L2 KO MEFs markedly repress NDUFA4 protein levels in hypoxia while Complex I activity is not affected, ruling out the possibility that Complex I activity is repressed in hypoxia via NDUFA4. These data stress the specific role of hypoxia-dependent NDUFA4L2 upregulation in Complex I activity inhibition.

DISCUSSION

The influence of fluctuations in oxygen concentration on mitochondrial activity has raised a great interest due to its broad impact on pathophysiology. Mitochondrial respiration is only compromised when the oxygen concentration drops below 0.1% O_2 because of the high affinity of mitochondrial cytochrome *c* oxidase (Complex IV) for oxygen (Aguirre et al., 2010; Gnaiger et al., 1998; Smolenski et al., 1991; Stumpe and Schrader, 1997). However, during moderate hypoxia (1%–2% O_2), cells

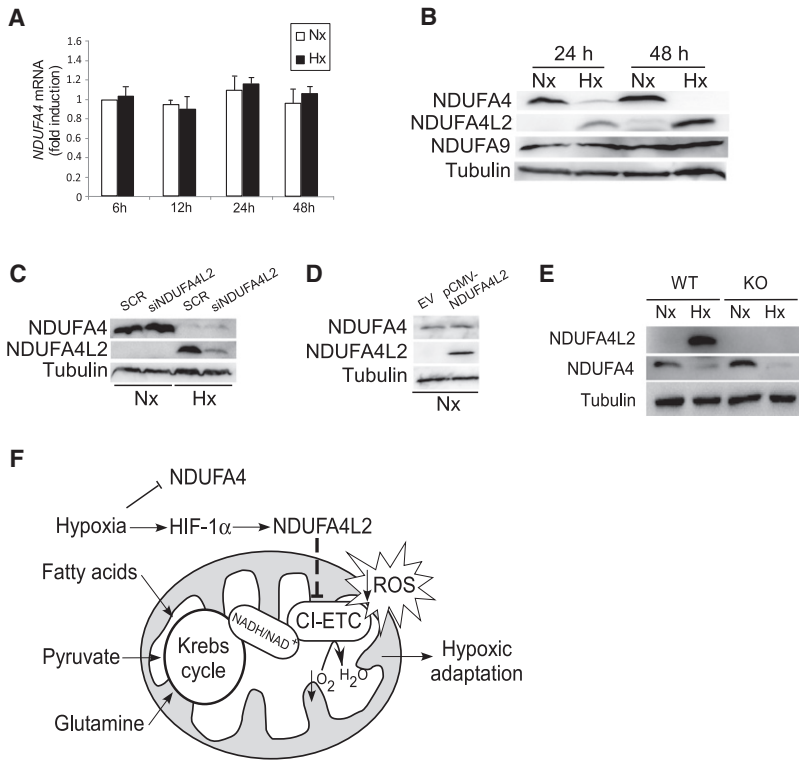

Figure 7. Opposite Regulation of NDUFA4 and NDUFA4L2 under Hypoxia

(A) HeLa cells were cultured under hypoxia (1% O_2) for 6, 12, 24, and 48 hr, and *NDUFA4* mRNA levels were analyzed.

(B) Immunoblot analysis of HeLa cells subjected to either 24 or 48 hr of hypoxia and proved against NDUFA4 and NDUFA4L2 antibodies. NDUFA9 was used as a loading control for Complex I, and tubulin was used as a total loading control.

(C and D) HeLa cells were transfected with a scramble control or NDUFA4L2 siRNA and then exposed to normoxic or hypoxic (1% O_2) conditions for 24 hr (C) or transfected with the empty or pCMV-NDUFA4L2 vector (D). Cell lysates were analyzed against NDUFA4, NDUFA4L2, and tubulin antibodies.

(E) Immunoblot analysis of MEFs WT and KO for NDUFA4L2 showing the total deficiency of NDUFA4L2 and the decrease of NDUFA4 under hypoxic (1% O_2) conditions for 24 hr. Tubulin was used as a loading control.

(F) Model showing the involvement of NDUFA4L2 induction by HIF-1α in hypoxic adaptation. HIF-1α stabilization by hypoxia upregulates NDUFA4L2, which inhibits ETC Complex I activity. As a result, oxygen consumption decreases and ROS production is abrogated, thereby allowing cells to adapt to the hypoxic conditions. In contrast, hypoxia decreases NDUFA4 protein levels ($n > 3$; mean ± SEM; $^*p < 0.05$; $^{**}p < 0.01$).

express a large number of genes, dependent on HIFs, that reprogram the metabolism to attenuate mitochondrial O_2 consumption, which also protects cells against excessive mitochondrial ROS formation (Aragonés et al., 2009; Kim et al., 2006; Papandreou et al., 2006).

At the molecular level, we show here that moderate hypoxia decreases oxygen consumption and Complex I activity via the HIF-1-dependent upregulation of NDUFA4L2. Our data indicate that *NDUFA4L2* is a HIF-1-dependent gene, emphasizing the role of HIF-1 in mitochondrial reprogramming and revealing NDUFA4L2 as an important element in metabolic adaptation to hypoxia. We have observed this induction in different cell types, as well as in tissue from animals subjected to hypoxia, suggesting a role in physiological adaptation to hypoxia. In this regard, NDUFA4L2 KO homozygous mice, which could be a presumed mouse model of Complex I gain of function based on our own data, show perinatal lethality, stressing the high relevance of this protein in vivo. Similarly, mouse models of Complex I deficiency (Kruse et al., 2008) also die shortly after birth, which indicates that Complex I activity needs to be tightly controlled to assure an adequate development early after birth.

The PHD oxygen-sensing pathway is also known to upregulate the PDH kinase isoforms PDK1, PDK3, and PDK4 (Aragonés et al., 2008; Kim et al., 2006; Lu et al., 2008; Papandreou et al., 2006). PDK overactivation reduces PDH activity, slowing down the conversion of pyruvate into acetyl-CoA and ultimately repressing the TCA cycle and the supply of NADH to the mitochondrial ETC. Therefore, PDKs could potentially cooperate with NDUFA4L2 to reduce mitochondrial Complex I activity under moderate hypoxic conditions, but it is also conceivable that NDUFA4L2 has other biological functions that cannot be accomplished by PDKs. For example, when metabolites that fuel the TCA cycle originate from pathways different from glycolysis (e.g., glutaminolysis or fatty acid oxidation), it would be necessary to reduce ETC activity in order to decrease mitochondrial function (Wheaton and Chandel, 2011). Hypoxia-induced NDUFA4L2 expression could fulfill this role, reducing oxygen consumption due to its strategic position downstream of the TCA cycle, possibly at Complex I (Figure 7F). Likewise, hypoxia induces the upregulation of microRNA-210, which represses ISCU1/2 (Chan et al., 2009; Chen et al., 2010; Favaro et al., 2010). These proteins facilitate the assembly of iron-sulfur clusters, including those in Complex I, Complex III, and aconitase, which are critical for electron transport and mitochondrial redox reactions. As a result, microRNA-210 represses mitochondrial respiration. In our model, and in line with previous studies, ISCU1/2 protein does not decrease prior to 48 hr and only under 0.5% O_2, while NDUFA4L2 becomes functional as early as 24 hr at 1% O_2. Moreover, ISCU1/2 recovery in hypoxic HeLa cells did not disturb proliferation. In this sense, it has been described that an anti-miR-210 affects HeLa cell proliferation at times longer than 48 hr and at very low oxygen tensions (0.01% O_2) (Favaro et al., 2010).

Very intriguingly, however, Complex I inhibition in HeLa cells takes place at milder hypoxia (1% O_2) (Figure 4), and this oxygen tension does not seem to be enough to decrease ISCU1/2 (Figure S5A). Furthermore, ISCU1/2 downregulation is not observed before 48 hr, but Complex I is inhibited as early as 24 hr. This opened a 24 hr window during which NDUFA4L2 could be acting before ISCU induction takes place. As demonstrated, NDUFA4L2 Complex I inhibition occurs without affecting Complex I quantity, but probably by a direct or indirect

interaction that remains to be elucidated. However, miRNA-210-targeted ISCU1/2 presumably fulfills its function by decreasing Complex I content. This early NDUFA4L2-dependent qualitative modulation followed by a later miR210-dependent quantitative repression of Complex I represents a possible model by which HIF-1 guarantees a fine control of Complex I under hypoxic conditions. In summary, we propose that, although NDUFA4L2 upregulation and miR-210-induced ISCU1/2 repression could act synergistically to decrease Complex I activity and oxygen consumption in chronic hypoxia, we should underscore that primary (1% O_2) Complex I inhibition can be only accomplished by early NDUFA4L2 induction.

Altered subunit content during hypoxia has also been reported for other ETC complexes. Thus, physiological hypoxia induces a COX4-1 to COX4-2 subunit switch, an effect mediated by HIF-1 that is thought to optimize the efficiency of respiration during conditions of reduced oxygen availability (Fukuda et al., 2007). Since we have found that NDUFA4 is downregulated at the protein level in hypoxia, we could speculate that NDUFA4L2 induction is taking over NDUFA4's place at Complex I and reducing in some way its activity. However, NDUFA4L2 KO MEFs markedly repress NDUFA4 protein levels in hypoxia, while Complex I activity is not affected, ruling out the possibility that Complex I activity is repressed in hypoxia via NDUFA4. In this regard, the role and location of NDUFA4 within Complex I are not yet well understood.

The ETC produces superoxide when single electrons are transferred to O_2 during electron transport. There are different sites of ROS production in mammalian mitochondria (Murphy, 2009), but the greatest maximum capacity of ROS production is the ubiquinone reduction site of Complex I and the outer quinone-binding site of the Q cycle in Complex III (Liu et al., 2002; Raha and Robinson, 2000; St-Pierre et al., 2002; Votyakova and Reynolds, 2001). Although superoxide production in isolated mitochondria correlates with oxygen tension (Liu et al., 2002), it is generally accepted that ROS production in cells increases during short periods of hypoxia (Brunelle et al., 2005; Guzy et al., 2005; Mansfield et al., 2005). In agreement with this, we detected increased ROS in hypoxia using the fluorescent probes DCFDA and MitoSOX. The hypoxia-induced ROS increase was exacerbated in the absence of NDUFA4L2, indicating that the expression of this protein keeps ROS production under control and hence could protect the cell against oxidative stress. Whether the effects of NDUFA4L2 on ROS production are direct or occur through the modulation of other mitochondrial proteins requires further research. However, the fact that mitochondrial membrane potential increases simultaneously with increased ROS in the absence of NDUFA4L2 suggests that both events might be closely associated, as has been demonstrated elsewhere (Korshunov et al., 1997; Votyakova and Reynolds, 2001).

Hypoxia-exposed cell cultures accumulate intracellular ROS, but most probably at lower sublethal concentrations. As shown in Figure 5, and in line with previous studies, hypoxia slows down proliferation (Gardner et al., 2001; Goda et al., 2003). However, NDUFA4L2-silenced cells and MEFs from NDUFA4L2 KO mice showed a more profound inhibition of cell proliferation in parallel to a higher ROS accumulation and DNA stress/damage (H2AX phosphorylation) than control cells or MEFs from wild-type mice. NDUFA4L2-silenced cells did not show signs of cellular apoptosis, probably because of the high-resistance nature of these tumor cells. Therefore, it is reasonable to think that the PHD-HIF system counteracts ROS overproduction that impairs cell growth.

Several in vivo and in vitro studies have revealed that the reduction of mitochondrial oxygen consumption through PHD and HIF activities prepares cells to tolerate more extreme lethal hypoxic/ischemic conditions, saving oxygen and reducing mitochondrial ROS formation. We hypothesize that NDUFA4L2 induction during hypoxia helps keep intracellular ROS production in check, consistent with the fact that NDUFA4L2 limits Complex I activity and prevents increases in membrane potential. It is therefore reasonable to speculate that NDUFA4L2 could participate in ischemic preconditioning. Indeed, several in vivo studies have shown that partial inhibition of Complex I with sublethal doses of amobarbital (a reversible inhibitor at the rotenone site of Complex I) prevents reperfusion-induced cardiac damage (Aldakkak et al., 2008; Chen et al., 2006a, 2006b).

Our studies indicate that mitochondrial Complex I activity is controlled by NDUFA4L2 during hypoxia. In conjunction with previous data on PHD- and HIF-regulated mitochondrial activity, we add further elements to the strategic armory used by HIFs to ensure that mitochondrial oxygen consumption is repressed in mild hypoxic conditions, highlighting the biological relevance of the regulation of this cellular response.

EXPERIMENTAL PROCEDURES

Cell Lines and Cultures

HeLa, RCC4, RCC4/VHL, PC-12, HL-1, neonatal rat cardiomyocytes, Hif-1$\alpha^{+/+}$/Cre or Hif-1$\alpha^{+f/+f}$/Cre MEFs, and human umbilical vein endothelial cells (HUVEC) were used. See Supplemental Experimental Procedures for details.

Microarray Analysis

Total RNA was extracted using Ultraspec reagent (Biotecx, Houston, TX). One-Color Microarray-Based Gene Expression Analysis Protocol (Agilent Technologies, Palo Alto, CA) was used to amplify and label RNA. Briefly, 200–700 ng of total RNA was reverse transcribed using T7 promoter Primer and MMLV-RT. Then cDNA was converted to aRNA using T7 RNA polymerase, which simultaneously amplifies target material and incorporates cyanine 3-labeled CTP. Samples were hybridized to Whole Human Genome Microarray 4 × 44K (G4112F, Agilent Technologies). Cy3-labeled aRNA (1.65 g) was hybridized for 17 hr at 65°C in a hybridization oven (G2545A, Agilent) set to 10 rpm in a final concentration of 1× GEx Hybridization Buffer HI-RPM, according to manufacturer's instructions (One-Color Microarray-Based Gene Expression Analysis, Agilent Technologies). Arrays were washed according to manufacturer's instructions (One-Color Microarray-Based Gene Expression Analysis, Agilent Technologies) and dried out using a centrifuge. Finally, arrays were scanned at 5 μm resolution on an Agilent DNA Microarray Scanner (G2565BA, Agilent Technologies) using the default settings for 4 × 44K format one-color arrays. Images provided by the scanner were analyzed using Feature Extraction software version 9.5.3.1 (Agilent Technologies).

In Vivo Hypoxia Experiments

Eight-week-old male C57BL/6 mice were exposed to hypoxic (7.5% O_2) or normoxic (21% O_2) conditions for 18 hr. After treatment mice were sacrificed under the same conditions to avoid tissue reoxygenation following hypoxia. The brain and heart were then excised, frozen in liquid nitrogen, and stored at −80°C. Organs were homogenized in liquid nitrogen and resuspended in RIPA buffer (1% NP40, 0.5% sodium deoxycholate, and 0.1% SDS in PBS buffer) for protein extraction or Ultraspec reagent (Biotecx, Houston, TX) for mRNA isolation.

Oxygen Consumption

Oxygen consumption was determined by high-resolution respirometry (Oxygraph-2k, Oroboros Instruments, Innsbruck, Austria). Cells were trypsinized after the indicated treatments and then resuspended at 2×10^6 cells/ml in HBSS containing 25 mM HEPES. The instrumental background flux was calculated as a linear function of the oxygen concentration, and the experimental data were corrected using DatLab software (Oroboros Instruments). The oxygen concentration in air-saturated culture medium at 37°C was 175.7 μM (Rodríguez-Juárez et al., 2007). Measurements were taken at 37°C in parallel Oxygraph-2k chambers for cells incubated in normoxic and hypoxic (1% O_2) conditions with the indicated treatments.

Mitochondria Isolation

The isolation of an enriched mitochondrial fraction from $2–5 \times 10^7$ HeLa cells was performed using the Mitochondria Isolation Kit MITOISO2 (Sigma) according to the manufacturer's instructions.

Complex I and IV Activity

The activities of Complex I and Complex IV were measured using the Complex I Enzyme Activity Microplate Assay Kit or the Complex IV Human Duplexing Microplate Assay Kit, both from MitoSciences, according to the manufacturer's instructions.

Mitochondrial Membrane Potential

Mitochondrial membrane potential was determined by incubating the cells with the fluorescent dye tetramethylrhodamine ethyl ester (TMRE; Sigma). Cells were incubated with 2.5 nM TMRE for 30 min at 37°C and subsequently analyzed by FACScan flow cytometer (Becton Dickinson, Lincoln Park, NJ).

Cell Proliferation and Apoptosis

For the cell proliferation assay, 2×10^5 HeLa, HUVEC, UCD-mel-N, and SKOV3 cells were planted in a 10 cm dish 1 day before exposure to hypoxic conditions (0.5% O_2). Either 0.1 mM NAC or 0.5 μM Mito-Q (0.5 μM DTPP was used as control of Mito-Q) was added to HeLa cells to determinate the effect of the antioxidants on NDUFA4L2-interfered cell proliferation in hypoxia. At the times indicated, the cells were trypsinized and the viable cells were counted using trypan blue. Apoptosis was determined by flow cytometry analysis of the cell cycle after DNA staining with propidium iodide (PI) and by analysis of cleaved caspase-3 with a specific antibody (Cell Signaling). Positive controls for apoptosis were performed by incubating HeLa cells with taxol (Calbiochem) at 1 μg/ml for 18 hr.

Soft Agar Assay

HeLa cells were seeded into 0.35% agar Noble (Difco) in DMEM containing 10% heat-inactivated FBS on top of a bed of 0.5% agar in 60 mm dishes at 5×10^3 cells per dish. Immobilized cells were grown for 15 days in a humidified chamber at 37°C and exposed to normoxic or hypoxic conditions (0.5% O_2). Colonies were then photographed using a DS-Fi1 camera (Nikon) and counted and measured using ImageJ software.

Analysis of ETC Complexes by Blue Native Electrophoresis Gel

Mitochondrial membrane proteins (100–150 mg) were applied and run on a 3%–13% first-dimension gradient Blue native electrophoresis gel as described elsewhere (Schägger, 1995). After electrophoresis, the complexes were electroblotted onto PVDF filters and sequentially probed with the following specific antibodies: anti-NDUFA9 (complex I), anti-core2 (complex III), anti-COI (complex IV), and anti-70 kDa subunit (complex II). All antibodies were obtained from Molecular Probes.

Ndufa4l2 Gene Inactivation in Mice

NDUFA4L2 chimeric males were obtained from Velocigene Regeneron Pharmaceuticals, Inc. (Reference number: 13661) through the KOMP repository. These chimeric mice were crossed with wild-type C57BL/6 females to generate NDUFA4L2 heterozygous mice. NDUFA4L2 heterozygous mice were used to generate NDUFA4L2-deficient embryos and the subsequent murine embryonic fibroblast isolation. The mice were bred and housed in a specific pathogen free (SPF) animal area of the animal facility at the Universidad Autónoma de Madrid (UAM).

Statistical Analysis

The data are presented as the means ± SEM of at least three independent experiments. Statistical significance *$p < 0.05$ or **$p < 0.01$ was assessed by the Wilcoxon test.

ACCESSION NUMBERS

The microarray data of HeLa cells are deposited at GEO DataSets with the accession number GSE33521.

SUPPLEMENTAL INFORMATION

Supplemental Information includes five figures, five tables, Supplemental Experimental Procedures, and Supplemental References and can be found with this article online at doi:10.1016/j.cmet.2011.10.008.

ACKNOWLEDGMENTS

This work was supported by Ministerio de Ciencia e Innovación (SAF 2007-06592, SAF 2010-14851), Comunidad Autónoma de Madrid (SAL 2006/0311), Metoxia Project-Health (F2 2009-222741), and Recava Network (RD 06/0014/0031) to M.O.L.; PS09/00101 and CP07/00143 to A.M.-R.; PI060701, PS09/00116, and CP08/00204 to S.C.; BFU2008-03407/BMC to J.A.; SAF2009-08007 to J.A.E.; and CSD2007-00020 to A.M.-R. and J.A.E. The CNIC is supported by the Instituto de Salud Carlos III-MICINN and the Pro-CNIC Foundation. We are grateful to Mike Murphy (Mitochondrial Biology Unit, MRC, Cambridge, UK) for the gift of MitoQ. We also thank Stephen Y. Chan and Joseph Loscalzo (Harvard Medical School, Boston, MA) for providing us ISCU expression vectors.

Received: April 12, 2010
Revised: July 21, 2011
Accepted: October 7, 2011
Published online: November 17, 2011

REFERENCES

Aguirre, E., Rodríguez-Juárez, F., Bellelli, A., Gnaiger, E., and Cadenas, S. (2010). Kinetic model of the inhibition of respiration by endogenous nitric oxide in intact cells. Biochim. Biophys. Acta *1797*, 557–565.

Aldakkak, M., Stowe, D.F., Chen, Q., Lesnefsky, E.J., and Camara, A.K. (2008). Inhibited mitochondrial respiration by amobarbital during cardiac ischaemia improves redox state and reduces matrix Ca2+ overload and ROS release. Cardiovasc. Res. *77*, 406–415.

Andreas, K., Häupl, T., Lübke, C., Ringe, J., Morawietz, L., Wachtel, A., Sittinger, M., and Kaps, C. (2009). Antirheumatic drug response signatures in human chondrocytes: potential molecular targets to stimulate cartilage regeneration. Arthritis Res. Ther. *11*, R15.

Aragonés, J., Schneider, M., Van Geyte, K., Fraisl, P., Dresselaers, T., Mazzone, M., Dirkx, R., Zacchigna, S., Lemieux, H., Jeoung, N.H., et al. (2008). Deficiency or inhibition of oxygen sensor Phd1 induces hypoxia tolerance by reprogramming basal metabolism. Nat. Genet. *40*, 170–180.

Aragonés, J., Fraisl, P., Baes, M., and Carmeliet, P. (2009). Oxygen sensors at the crossroad of metabolism. Cell Metab. *9*, 11–22.

Brunelle, J.K., Bell, E.L., Quesada, N.M., Vercauteren, K., Tiranti, V., Zeviani, M., Scarpulla, R.C., and Chandel, N.S. (2005). Oxygen sensing requires mitochondrial ROS but not oxidative phosphorylation. Cell Metab. *1*, 409–414.

Carroll, J., Fearnley, I.M., Skehel, J.M., Shannon, R.J., Hirst, J., and Walker, J.E. (2006). Bovine complex I is a complex of 45 different subunits. J. Biol. Chem. *281*, 32724–32727.

Chan, S.Y., Zhang, Y.Y., Hemann, C., Mahoney, C.E., Zweier, J.L., and Loscalzo, J. (2009). MicroRNA-210 controls mitochondrial metabolism during hypoxia by repressing the iron-sulfur cluster assembly proteins ISCU1/2. Cell Metab. *10*, 273–284.

Chen, Q., Hoppel, C.L., and Lesnefsky, E.J. (2006a). Blockade of electron transport before cardiac ischemia with the reversible inhibitor amobarbital protects rat heart mitochondria. J. Pharmacol. Exp. Ther. *316*, 200–207.

Chen, Q., Moghaddas, S., Hoppel, C.L., and Lesnefsky, E.J. (2006b). Reversible blockade of electron transport during ischemia protects mitochondria and decreases myocardial injury following reperfusion. J. Pharmacol. Exp. Ther. *319*, 1405–1412.

Chen, Z., Li, Y., Zhang, H., Huang, P., and Luthra, R. (2010). Hypoxia-regulated microRNA-210 modulates mitochondrial function and decreases ISCU and COX10 expression. Oncogene *29*, 4362–4368.

Driessens, N., Versteyhe, S., Ghaddhab, C., Burniat, A., De Deken, X., Van Sande, J., Dumont, J.E., Miot, F., and Corvilain, B. (2009). Hydrogen peroxide induces DNA single- and double-strand breaks in thyroid cells and is therefore a potential mutagen for this organ. Endocr. Relat. Cancer *16*, 845–856.

Favaro, E., Ramachandran, A., McCormick, R., Gee, H., Blancher, C., Crosby, M., Devlin, C., Blick, C., Buffa, F., Li, J.L., et al. (2010). MicroRNA-210 regulates mitochondrial free radical response to hypoxia and krebs cycle in cancer cells by targeting iron sulfur cluster protein ISCU. PLoS ONE *5*, e10345.

Favier, J., Brière, J.J., Burnichon, N., Rivière, J., Vescovo, L., Benit, P., Giscos-Douriez, I., De Reyniès, A., Bertherat, J., Badoual, C., et al. (2009). The Warburg effect is genetically determined in inherited pheochromocytomas. PLoS ONE *4*, e7094.

Fredlund, E., Ovenberger, M., Borg, K., and Påhlman, S. (2008). Transcriptional adaptation of neuroblastoma cells to hypoxia. Biochem. Biophys. Res. Commun. *366*, 1054–1060.

Frost, M.T., Wang, Q., Moncada, S., and Singer, M. (2005). Hypoxia accelerates nitric oxide-dependent inhibition of mitochondrial complex I in activated macrophages. Am. J. Physiol. Regul. Integr. Comp. Physiol. *288*, R394–R400.

Fukuda, R., Zhang, H., Kim, J.W., Shimoda, L., Dang, C.V., and Semenza, G.L. (2007). HIF-1 regulates cytochrome oxidase subunits to optimize efficiency of respiration in hypoxic cells. Cell *129*, 111–122.

Gardner, L.B., Li, Q., Park, M.S., Flanagan, W.M., Semenza, G.L., and Dang, C.V. (2001). Hypoxia inhibits G1/S transition through regulation of p27 expression. J. Biol. Chem. *276*, 7919–7926.

Gnaiger, E., Lassnig, B., Kuznetsov, A.V., and Margreiter, R. (1998). Mitochondrial respiration in the low oxygen environment of the cell. Effect of ADP on oxygen kinetics. Biochim. Biophys. Acta *1365*, 249–254.

Goda, N., Ryan, H.E., Khadivi, B., McNulty, W., Rickert, R.C., and Johnson, R.S. (2003). Hypoxia-inducible factor 1alpha is essential for cell cycle arrest during hypoxia. Mol. Cell. Biol. *23*, 359–369.

Guzy, R.D., Hoyos, B., Robin, E., Chen, H., Liu, L., Mansfield, K.D., Simon, M.C., Hammerling, U., and Schumacker, P.T. (2005). Mitochondrial complex III is required for hypoxia-induced ROS production and cellular oxygen sensing. Cell Metab. *1*, 401–408.

Iyer, N.V., Kotch, L.E., Agani, F., Leung, S.W., Laughner, E., Wenger, R.H., Gassmann, M., Gearhart, J.D., Lawler, A.M., Yu, A.Y., and Semenza, G.L. (1998). Cellular and developmental control of O2 homeostasis by hypoxia-inducible factor 1 alpha. Genes Dev. *12*, 149–162.

Kaelin, W.G., Jr., and Ratcliffe, P.J. (2008). Oxygen sensing by metazoans: the central role of the HIF hydroxylase pathway. Mol. Cell *30*, 393–402.

Kim, J.W., Tchernyshyov, I., Semenza, G.L., and Dang, C.V. (2006). HIF-1-mediated expression of pyruvate dehydrogenase kinase: a metabolic switch required for cellular adaptation to hypoxia. Cell Metab. *3*, 177–185.

Korshunov, S.S., Skulachev, V.P., and Starkov, A.A. (1997). High protonic potential actuates a mechanism of production of reactive oxygen species in mitochondria. FEBS Lett. *416*, 15–18.

Kruse, S.E., Watt, W.C., Marcinek, D.J., Kapur, R.P., Schenkman, K.A., and Palmiter, R.D. (2008). Mice with mitochondrial complex I deficiency develop a fatal encephalomyopathy. Cell Metab. *7*, 312–320.

Liu, Y., Fiskum, G., and Schubert, D. (2002). Generation of reactive oxygen species by the mitochondrial electron transport chain. J. Neurochem. *80*, 780–787.

Lu, C.W., Lin, S.C., Chen, K.F., Lai, Y.Y., and Tsai, S.J. (2008). Induction of pyruvate dehydrogenase kinase-3 by hypoxia-inducible factor-1 promotes metabolic switch and drug resistance. J. Biol. Chem. *283*, 28106–28114.

Mansfield, K.D., Guzy, R.D., Pan, Y., Young, R.M., Cash, T.P., Schumacker, P.T., and Simon, M.C. (2005). Mitochondrial dysfunction resulting from loss of cytochrome c impairs cellular oxygen sensing and hypoxic HIF-alpha activation. Cell Metab. *1*, 393–399.

Murphy, M.P. (2009). How mitochondria produce reactive oxygen species. Biochem. J. *417*, 1–13.

Papandreou, I., Cairns, R.A., Fontana, L., Lim, A.L., and Denko, N.C. (2006). HIF-1 mediates adaptation to hypoxia by actively downregulating mitochondrial oxygen consumption. Cell Metab. *3*, 187–197.

Piruat, J.I., and López-Barneo, J. (2005). Oxygen tension regulates mitochondrial DNA-encoded complex I gene expression. J. Biol. Chem. *280*, 42676–42684.

Raha, S., and Robinson, B.H. (2000). Mitochondria, oxygen free radicals, disease and ageing. Trends Biochem. Sci. *25*, 502–508.

Rodríguez-Juárez, F., Aguirre, E., and Cadenas, S. (2007). Relative sensitivity of soluble guanylate cyclase and mitochondrial respiration to endogenous nitric oxide at physiological oxygen concentration. Biochem. J. *405*, 223–231.

Schägger, H. (1995). Native electrophoresis for isolation of mitochondrial oxidative phosphorylation protein complexes. Methods Enzymol. *260*, 190–202.

Schofield, C.J., and Ratcliffe, P.J. (2004). Oxygen sensing by HIF hydroxylases. Nat. Rev. Mol. Cell Biol. *5*, 343–354.

Semenza, G.L. (2004). Hydroxylation of HIF-1: oxygen sensing at the molecular level. Physiology (Bethesda) *19*, 176–182.

Semenza, G.L. (2009). Regulation of oxygen homeostasis by hypoxia-inducible factor 1. Physiology (Bethesda) *24*, 97–106.

Smolenski, R.T., Schrader, J., de Groot, H., and Deussen, A. (1991). Oxygen partial pressure and free intracellular adenosine of isolated cardiomyocytes. Am. J. Physiol. *260*, C708–C714.

St-Pierre, J., Buckingham, J.A., Roebuck, S.J., and Brand, M.D. (2002). Topology of superoxide production from different sites in the mitochondrial electron transport chain. J. Biol. Chem. *277*, 44784–44790.

Stumpe, T., and Schrader, J. (1997). Phosphorylation potential, adenosine formation, and critical PO2 in stimulated rat cardiomyocytes. Am. J. Physiol. *273*, H756–H766.

Vogel, R.O., Janssen, R.J., Ugalde, C., Grovenstein, M., Huijbens, R.J., Visch, H.J., van den Heuvel, L.P., Willems, P.H., Zeviani, M., Smeitink, J.A., and Nijtmans, L.G. (2005). Human mitochondrial complex I assembly is mediated by NDUFAF1. FEBS J. *272*, 5317–5326.

Votyakova, T.V., and Reynolds, I.J. (2001). DeltaPsi(m)-Dependent and -independent production of reactive oxygen species by rat brain mitochondria. J. Neurochem. *79*, 266–277.

Walker, J.E., Arizmendi, J.M., Dupuis, A., Fearnley, I.M., Finel, M., Medd, S.M., Pilkington, S.J., Runswick, M.J., and Skehel, J.M. (1992). Sequences of 20 subunits of NADH:ubiquinone oxidoreductase from bovine heart mitochondria. Application of a novel strategy for sequencing proteins using the polymerase chain reaction. J. Mol. Biol. *226*, 1051–1072.

Wheaton, W.W., and Chandel, N.S. (2011). Hypoxia. 2. Hypoxia regulates cellular metabolism. Am. J. Physiol. Cell Physiol. *300*, C385–C393.